PERGAMON

Available online at www.sciencedirect.com
ScienceDirect

Acta Astronautica 65 (2009) 792–803

ACTA ASTRONAUTICA

www.elsevier.com/locate/actaastro

Passive magnetic attitude stabilization of the UNISAT-4 microsatellite

Fabio Santoni*, Mauro Zelli

Scuola di Ingegneria Aerospaziale, University of Rome "La Sapienza", Via Eudossiana, 18, 00184 ROMA, Italy

Received 13 June 2007; accepted 5 March 2009
Available online 7 April 2009

Abstract

UNISAT-4 is the fourth educational microsatellite, completely designed and built by students and professors of the research group GAUSS (Gruppo di Astrodinamica dell'Università degli Studi "la Sapienza") at the Scuola di Ingegneria Aerospaziale of University of Rome "La Sapienza". The spacecraft is stabilized using a passive magnetic attitude stabilization system, based on a permanent magnet and an energy dissipation system, which consists of magnetic hysteresis rods. The main features of passive magnetic stabilization are simplicity and reliability. However, sizing the system parameters, predicting the in-orbit performance and obtainable accuracy of passive magnetic stabilization systems is not trivial. The main problem in the system design is accurate modeling of the hysteresis rods magnetization and the evaluation of the rods magnetic parameters, such as apparent permeability, remanence and coercitive force, which are considerably affected by the rods' manufacturing technological process. In this paper the design and ground test of the UNISAT-4 magnetic attitude stabilization system is described. A method to experimentally determine the hysteresis rod parameters is described and an accurate model of the satellite dynamics is obtained, based on the results of the measurements. One of the main design parameters is the number of hysteresis rods necessary to obtain satellite stabilization. Numerical simulations for two hysteresis rods per axis and eight hysteresis rods per axis are discussed, showing that the satellite stabilizes in about 14 days, with a residual oscillation amplitude of less than 10°, if eight rods are used.

1. Introduction

The education and research program UNISAT was established by the research group Gruppo di Astrodinamica dell'Università degli Studi "la Sapienza" (GAUSS) at the Scuola di Ingegneria Aerospaziale of University of Rome "La Sapienza" [1–4]. UNISAT-4, shown in Fig. 1, is the fourth education microsatellite of the UNISAT program, completely designed and built by students and professors of GAUSS. It is basically an improved version of the microsatellite UNISAT-3, successfully launched and operative in orbit for almost 3 years. The satellite bus is the same, while the main subsystems, namely power, communication and on-board data handling are improvements on the ones tested on UNISAT-3.

UNISAT-4's aim is testing in orbit some technological components [5], namely terrestrial technology and triple junction solar panels, commercial cameras to take pictures of the Earth, commercial fluxgate and magnetoresistive three-axis magnetometers, S-band communication link, an MPPT (maximum peak power tracking) system, the on-board data handling system [4,5], based on a COTS embedded system for terrestrial robotic application, and a re-entry system to de-orbit the satellite (SIRDARIA), useful for space debris mitigation[6]. The satellite also hosts a small scientific experiment, consisting of a triple Langmuir probe to measure the

* Corresponding author. Tel.: +39 644585328; fax: +39 644585952.
E-mail addresses: fabio.santoni@uniroma1.it (F. Santoni), mauro.zl@libero.it (M. Zelli).

0094-5765/$ - see front matter © 2009 Elsevier Ltd. All rights reserved.
doi:10.1016/j.actaastro.2009.03.012

Nomenclature

A	satellite transverse moment of inertia
B_0	remanence of permeable rod
B_m	saturation flux density of permeable rod
B_r	magnetic flux density of permeable rod
B_c	magnetic flux density along the centerline of permeable rod
B_{eq}	Earth's magnetic flux density in orbit at the equator
$B_{\min}$	minimum Earth's magnetic flux density in orbit
B_s	hysteresis rod material saturation magnetic flux density
B'_s	effective hysteresis rod saturation magnetic flux density
$\vec{B}$	Earth magnetic flux density in orbit
C	satellite moment of inertia around the permanent magnet axis
D	hysteresis rod magnetic dipole
H	magnetic field along the permeable rod direction
H_0	coercitive force of permeable rod
H_s	hysteresis rod material saturation magnetic field
H'_s	effective hysteresis rod saturation magnetic field
l	hysteresis rod length
k	parametric resonance index
m	hysteresis rod elongation ($m = l/s$)
M	permanent magnet magnetic dipole intensity
$\vec{M}$	permanent magnet magnetic dipole vector
N	permeable rod demagnetizing factor
n_0	orbit mean motion
r_c	distance from the rod center along the rod centerline
s	hysteresis rod cross section side
S	hysteresis rod cross section area
T_{sum}	satellite total maximum environmental torque
$\vec{T}_{pm}$	torque due to permanent magnet
z	abscissa along rod centerline
$\beta_{\max}$	satellite pointing accuracy (angle between Earth magnetic field and permanent magnet dipole axis after stabilization is reached)
η	parametric resonance parameter
$\eta_\perp$	parametric resonance parameter
λ	moment of inertia ratio $\lambda = C/A$
μ_0	permeability of vacuum
μ_r	hysteresis rod true permeability
μ'_r	hysteresis rod apparent permeability
χ	hysteresis rod material susceptivity

plasma density in orbit [7]. The UNISAT-4 orbit is circular, sun-synchronous, and 500 km high.

The attitude control system design and manufacturing follows the UNISAT program philosophy of fast development (about 1.5 years from concept to launch) and low cost. The attitude stabilization system, which responds better to the overall program requirements, is a passive magnetic attitude stabilization system based on a permanent magnet and an energy dissipation system. For UNISAT-4, it consists of eight magnetic hysteresis rods per axis based on the system design described in this paper.

A detailed passive magnetic stabilization system design procedure can be found in Refs. [8,9], where an approximate solution of the attitude dynamics equations is obtained introducing simplifying assumptions and using the averaging technique. It is shown that parametric resonance may occur due to the periodic coefficient equations of motion. The permeable rods sizing, location inside the satellite and mutual demagnetization are discussed and the system validated through numerical simulation.

The passive magnetic attitude stabilization system design of UNISAT-4 is performed basically following the steps suggested in Refs. [8,9]. The hysteresis rod parameters are greatly affected by the manufacturing process and heat treatment, which cannot be theoretically predicted. A simple experimental setup is described in this paper to evaluate the actual hysteresis rod parameters and verify that the design requirements are satisfied. The motivation for this work starts from the experience gained with the satellite UNISAT-3, operative in orbit for about 3 years, which has a passive magnetic attitude stabilization system, similar to UNISAT-4. The UNISAT-3 hysteresis rods parameters were not measured after the manufacturing process.

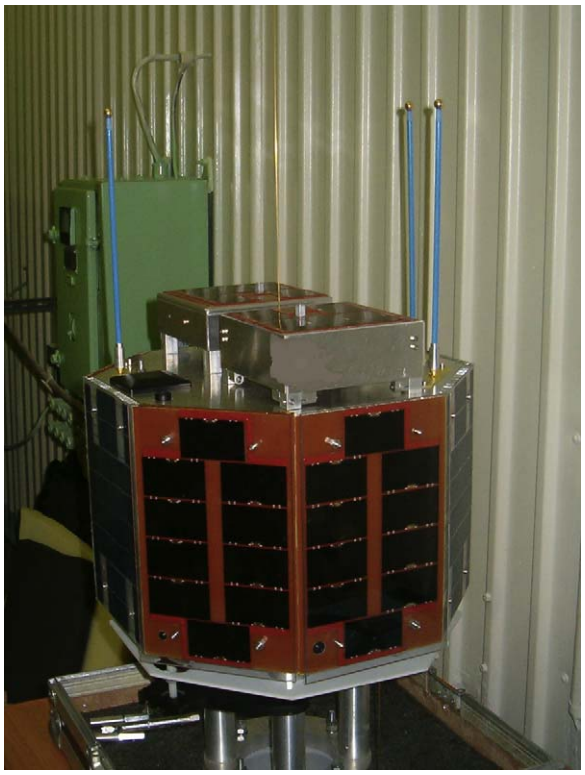

Fig. 1. UNISAT-4.

Data collected in orbit show that the satellite oscillation amplitude about the magnetic field is in the order of 30° [10]. This might be due to the poor performance of the hysteresis rods and this is why the procedure described in this paper has been set up.

2. UNISAT-4 attitude stabilization system

UNISAT-4 is stabilized using a passive magnetic attitude stabilization system consisting of a permanent magnet aligned with the satellite axis of symmetry and hysteresis rods. The permanent magnet dipole interacts with the geomagnetic field, producing a restoring torque which aligns satellite axis of symmetry with Earth's magnetic field. Because of the orbital motion, the magnetic field direction is not constant. This forces the satellite to oscillate around the magnetic field and the oscillations amplitude must be controlled by energy dissipation. In UNISAT-4 energy dissipation is provided by eight hysteresis rods per axis in the equatorial plane of the permanent magnet. The permeable rod system provides also for the dissipation of the initial attitude kinetic energy at separation from the launcher.

Table 1
Environmental torques.

Torque	Value (Nm)
Aerodynamic	8×10^{-8}
Gravity gradient	4×10^{-8}
Solar pressure	1×10^{-8}
Residual magnetic dipole	1×10^{-8}
Worst case total	1.4×10^{-7}

The expected satellite attitude motion is similar to an oscillating compass needle providing two turns per orbit in near polar orbits.

2.1. Permanent magnet sizing

The permanent magnet torque is

$$\vec{T}_{pm} = \vec{M} \times \vec{B} \tag{1}$$

The permanent magnet dipole must be such that the magnetic torque is much larger than the other environmental torques, when the angle between the magnetic dipole and the Earth's magnetic field is in the order of the expected attitude stabilization system accuracy, which for UNISAT-4 is about 10°. The evaluation of the UNISAT-4 environmental torques is given in Table 1.

The magnetic dipole is evaluated providing for a restoring torque, 30 times the worst case sum of all the environmental torques; thus,

$$M = 30\frac{T_{sum}}{B_{\min}\sin(\beta_{\max})} \tag{2}$$

where T_{sum} is the sum of all the environmental torques (Table 1), B_{min} is the minimum value of the Earth's magnetic field at 500 km (2.44×10^{-5} T) and $\beta_{\max}$ the expected pointing accuracy (10°). The resulting necessary magnetic dipole is in the order of 1 A m^2.

In near polar orbits parametric resonance may occur, as discussed in Refs. [8,9]. The parametric resonance depends on two satellite parameters: $\eta=(MB_{eq})/(An_0)$; $\lambda = C/A$. There are in-plane resonances as well as out-of-plane resonances, depending on these two parameters.

The formulae giving the resonance are

$$\eta \cong 2.63k^2 - 0.49 + 0.51\lambda$$
$$\eta_\perp \cong 2.63k^2 - 4.25 + 1.25\lambda \tag{3}$$

with k integer and the subscript $\perp$ indicating the out-of-plane resonance. The values of η and λ obtained by (3) for UNISAT-4 are listed in Table 2 ($A = 0.11$ kg m^2, $C = 0.13$ kg m^2, orbit height: 500 km).

Table 2
Values of M for parametric resonance.

k	η	$\eta_\perp$	M	$M_\perp$
1	2.723514	−0.190	0.015	
2	10.61351	7.700	0.059	0.043
3	23.76351	20.850	0.132	0.116
4	42.17351	39.260	0.235	0.219
5	65.84351	62.930	0.367	0.351
6	94.77351	91.860	0.528	0.512
7	128.9635	126.050	0.718	0.702
8	168.4135	165.500	0.938	0.922
9	213.1235	210.210	1.187	1.171
10	263.0935	260.180	1.466	1.449

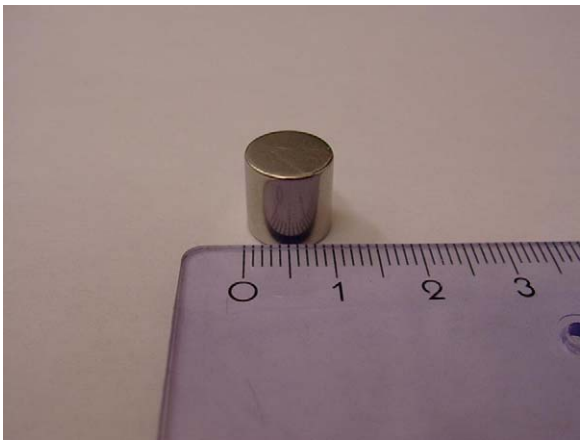

Fig. 2. UNISAT-4 on-board permanent magnet.

The value $M = 1\,\mathrm{Am}^2$ is between the parametric resonances $k = 8$ and $k = 9$, quite far from parametric resonance. Numerical simulations confirmed that resonance does not occur, as discussed in Section 5.

Fig. 2 shows the commercial permanent magnet installed on UNISAT-4. The magnetic dipole of one magnet is about $0.06\,\mathrm{A\,m}^2$. Sixteen magnets are on-board the satellite to reach the required magnetic dipole of $1\,\mathrm{A\,m}^2$.

2.2. Hysteresis rod sizing

A short discussion of well known relations used for the hysteresis rod magnetic dipole evaluation is given, to clarify the assumptions made and evaluate the hysteresis rod performance.

A simple mathematical model of the hysteresis rod magnetic dipole can be obtained assuming that the magnetization within the rod is parallel to the external magnetic field. This is true for ellipsoid shaped bodies, and can be considered a valid approximation for very elongated bodies [11].

The rod magnetic dipole D is given by

$$D = B_r V \tag{4}$$

where B_r is the magnetic flux intensity within the rod and V the rod volume. B_r is proportional to the magnetic field component parallel to the rod:

$$B_r = \mu_0 \mu_r' H \tag{5}$$

in which H is the magnetic field, μ_0 the permeability of vacuum and μ_r' the apparent permeability, depending on the rod material's true permeability μ_r and the demagnetizing factor N:

$$\mu_r' = \frac{\mu_r(H)}{1 + N\mu_r(H)} \tag{6}$$

μ_r depends on the rod material magnetization history and the magnetizing field H itself, while N depends on the rod material susceptivity χ, on the rod shape (e.g. circular, square or rectangular cross section) and on the elongation m.

The relation between N, m and χ is evaluated using approximate analytical solutions or by numerical methods (e.g. finite elements method). Soft magnetic material susceptivity can be assumed as infinity. Tabulated values and empirical approximating relations can be found in literature. The expressions given in Refs. [12–14] are reported in Appendix A. The resulting values for the demagnetization factor and apparent permeability are shown in Figs. 3 and 4. It is evident that accurate prediction of the rod demagnetization factor and true permeability is not trivial and depends strongly on the assumptions made. In Fig. 4, we notice that the apparent permeability reaches a steady state value when the true permeability increases. The demagnetizing effect is evident, showing that a maximum apparent permeability between 300 and 350 is reached. Thus, improving the material permeability does not correspondingly improve the rod performance.

The rod magnetic dipole per unit volume represents the rod efficiency and it is the main parameter to be considered for sizing the rod. It is intuitive that maximum efficiency is obtained for very elongated rods. This can be easily shown considering that the Earth's magnetic field is not strong enough to take the rod to saturation. In this assumption one can remove the dependence of μ_r by H in (6). The simplest expression of N is [13]

$$N = \frac{1}{1 + 2m} \tag{7}$$

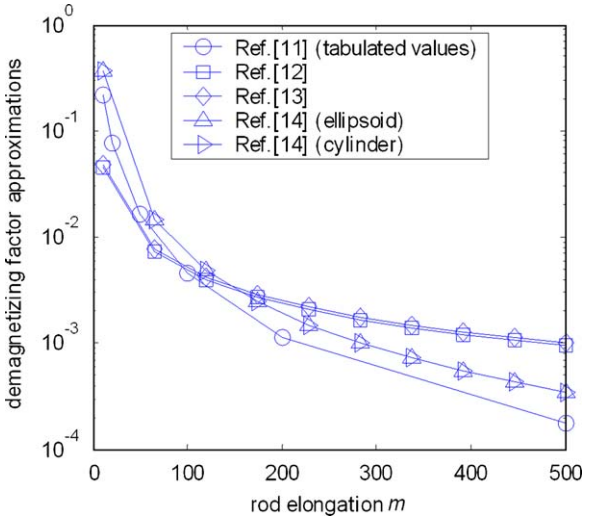

Fig. 3. Hysteresis rod demagnetization factor according to different references.

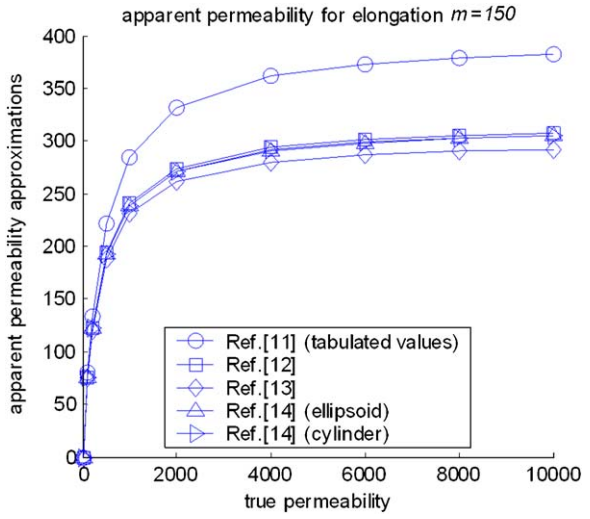

Fig. 4. Hysteresis rod apparent permeability.

Combining Eqs. (3)–(7), and considering that practical values of the rod elongation are in the order of 100 and that μ_r is in the order of 10^4, we obtain

$$\frac{D}{V} = B_r = \mu_0 \mu_r H \frac{(1+2m)}{(1+\mu_r)+2m} \simeq 2m\mu_0 H \tag{8}$$

which confirms that the efficiency is approximately proportional to the bar elongation. The rod length is limited by the satellite geometry, so one can only reduce the rod cross section side to improve efficiency. A lower limit to the rod cross section is given by the effective dipole obtained, which is proportional to the volume.

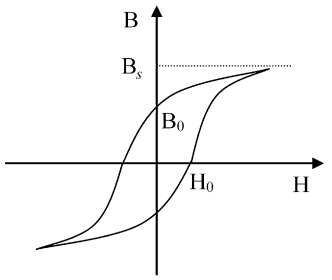

Fig. 5. Hysteresis loop parameter definition.

Obviously, making the rod too thin gives too small a dipole. Typically many bars parallel to each other are used to improve the magnetic dipole, while maintaining a good rod efficiency. Bar mutual demagnetization can be neglected when the distance between bars is about one third of the length [15]. Therefore, the rods sizing is mainly based on practical considerations, to obtain the best compromise out of these different effects.

The UNISAT-4 rod length is fixed to 15 cm by the room available inside the satellite. The rod cross section side has been chosen by a compromise between the magnetic dipole efficiency, the rod structural robustness and manufacturing process (see following section). It has been fixed to 1 mm, and then the appropriate number of bars has been evaluated to obtain the magnetic stabilization in about 14 days, as discussed in Section 5.

Many mathematical models are available in literature to describe the hysteresis loop of soft magnetic materials. In this paper we use the model described in Ref. [16]. The approximating equation for the major hysteresis loop is

$$B_r = (2B_s/\pi)\tan^{-1}[k(H \pm H_0)] \tag{9}$$

where + and − are the left and right side of the loop, respectively, and $k = \tan[(\pi B_0/2B_s)/H_0]$. The hysteresis loop parameter definition is shown in Fig. 5.

Eq. (9) describes the hysteresis loop of the material as given by the manufacturer, as well as the hysteresis loop of material specimens of any particular shape. In the first case, the loop parameters refer to an ideal hysteresis loop obtained in a magnetic circuit without air gaps [17]. In the second case, the parameters depend on the material properties and specimen shape. The permeable rod hysteresis loop parameters are affected by demagnetization; therefore, accurate predictions cannot be performed, for the above stated reasons. A procedure to evaluate these parameters using a simple experimental setup is described in Section 4.

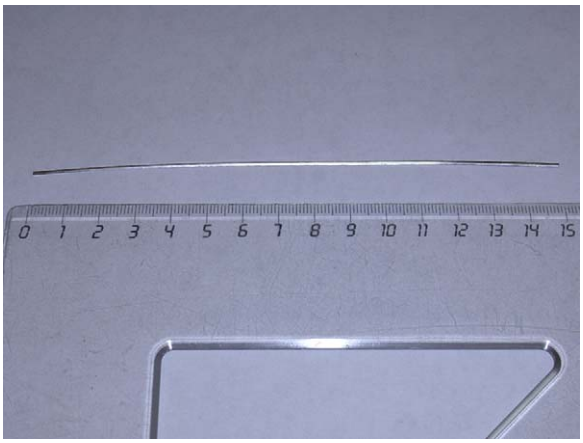

Fig. 6. UNISAT-4 hysteresis rod.

Fig. 7. UNISAT-4 hysteresis rod encapsulated in a vacuum glass tube for thermal treatment.

3. Hysteresis rod manufacturing

The UNISAT-4 hysteresis rods have been manufactured using commercial soft magnetic material, namely a 79% Ni, 4% Mo, 17% Fe alloy. The bars have been obtained cutting a 1 mm thickness laminate in strips of 1 mm. The resulting rod is shown in Fig. 6. The rod weight is 1.35 g.

The rods have been heat treated according to the manufacturer's suggestions, in order to remove the effects of the mechanical stress originating from the cutting process. Fig. 7 shows the bar encapsulated in an evacuated glass tube before undergoing heat treatment. Fig. 8 shows the extraction of the bars from the high-temperature oven.

Fig. 8. Thermal treatment of the hysteresis rod in high-temperature oven.

4. Hysteresis rod parameter measurement

The hysteresis rod parameters have been experimentally evaluated. Testing equipment is commercially available to accurately measure the magnetic properties of soft magnetic materials. These tests are aimed at evaluating the material ideal hysteresis loop parameters and therefore emphasize measurement of basic material properties. Appropriate standardized methods have been established, defining the material specimen size, shape and magnetic circuit configuration, so that manufacturers and users have common methods to determine material properties [17]. These kinds of tests do not refer to any particular requirements of the material under test final application. In the case of the UNISAT-4 hysteresis rod, we are interested in the determination of the final rod properties, including the effect of demagnetization and in the presence of magnetizing fields in the order of 45 A/m, which is the maximum Earth's magnetic field intensity in an orbit of 500 km height.

A measurement setup has been designed and realized to evaluate the final hysteresis rod magnetic properties. The rod is exposed to a known magnetizing field and the consequent magnetic flux density is measured by a fluxgate magnetometer aligned with the rod. The measurement setup block diagram and hardware realization are shown in Figs. 9 and 10, respectively. The rod under test is posed in the centerline of a solenoid, generating the magnetizing field. The solenoid is obtained winding a 0.1 mm diameter magnet wire on square aluminum bar. The solenoid length necessary to test the 15 cm rod is evaluated so that the magnetic field strength is approximately constant over the rod length. The solenoid cross section side is 1 cm, the solenoid length 20 cm.

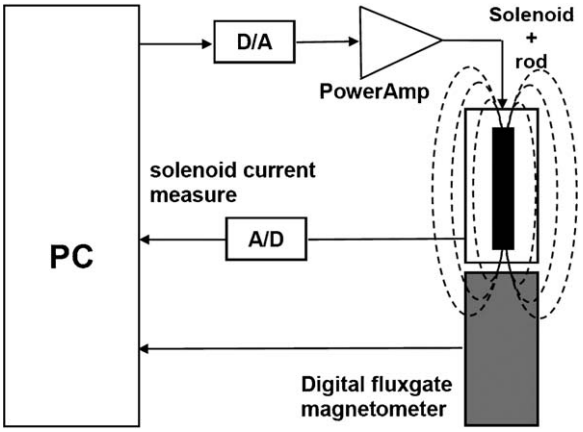

Fig. 9. Experimental setup block diagram.

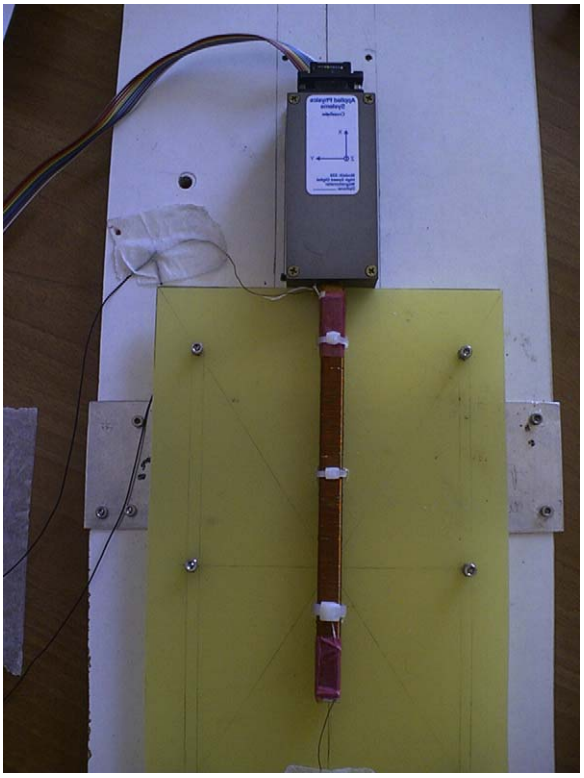

Fig. 10. Measurement set-up.

The magnetic field strength at the solenoid centerline is shown in Fig. 11. It is approximately constant over about 7.5 cm of half the length of the solenoid.

The solenoid current is controlled by a personal computer using a digital to analog conversion system and a power amplifier. It is measured using an analog to digital conversion system. This feedback loop ensures that

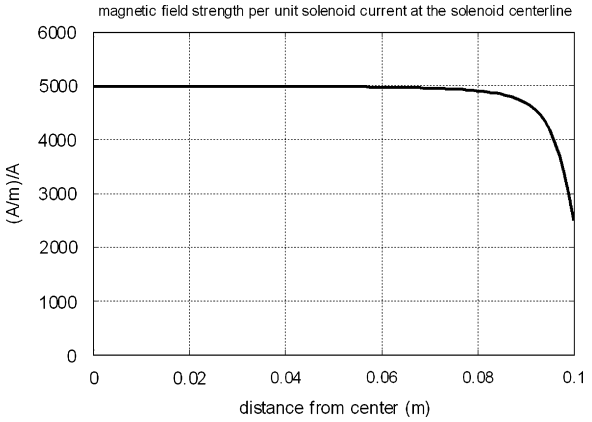

Fig. 11. Magnetizing field intensity inside the solenoid.

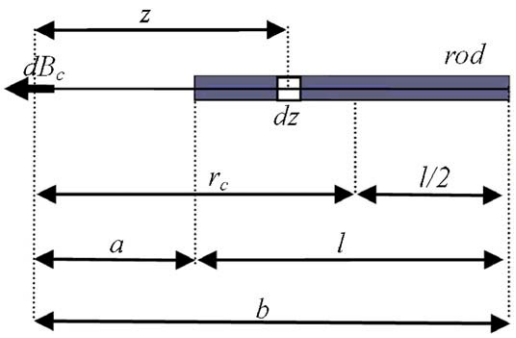

Fig. 12. Evaluation of the magnetic flux intensity on the rod centerline.

the prefixed current is actually going into the solenoid. The permeable rod magnetic flux intensity is measured by a magnetometer aligned with the rod, exploiting the relation between the rod magnetization and the magnetic flux intensity outside the rod. This relation can be obtained as follows. We assume that the magnetic field inside the rod B_r is homogenous and equal to the magnetic field in the rod centerline. Introducing the abscissa z on the rod centerline, the magnetic field generated by the element dz at distance z along the rod centerline (Fig. 12) is

$$dB_c = 2\frac{B_r S dz}{z^3} \tag{10}$$

The magnetic flux density is then obtained integrating between a and b:

$$B_c = S\left(\frac{1}{a^2} - \frac{1}{b^2}\right) B_r \tag{11}$$

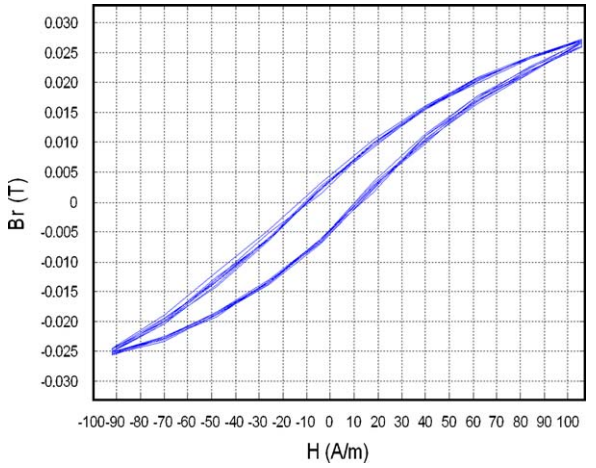

Fig. 13. UNISAT-4 permeable rods, measured apparent hysteresis loops.

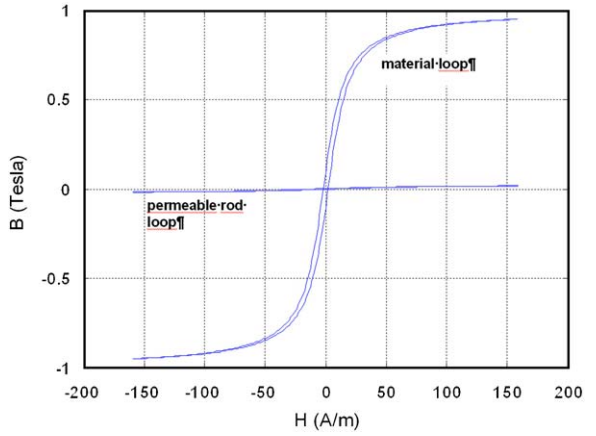

Fig. 14. UNISAT-4 permeable rods, ideal and apparent hysteresis loops.

It can be expressed in terms of the bar length and the distance measured from the rod center:

$$B_c = S\frac{2r_c l}{r_c^2 - (l/2)^2}B_r \tag{12}$$

The magnetic flux density B_c is measured using a magnetometer with the sensing element on the hysteresis rod centerline and the flux inside the permeable rod can be determined using (11) or (12). Substituting in (11) the values for the UNISAT-4 measurement setup $a = 34\,\text{mm}$, $b = 184\,\text{mm}$, $S = 1\,\text{mm}^2$, we get $B_r = 1.197 \times 10^3 B_c$.

The results of the measurements are shown in Fig. 13, representing the permeable rod major hysteresis loop. The rod saturation magnetic flux is about 0.025 T, as

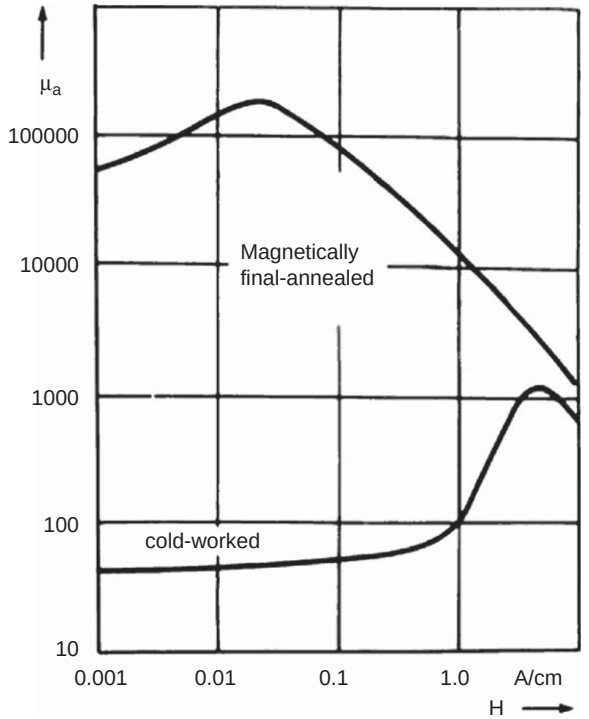

Fig. 15. Permeable rod material true permeability.

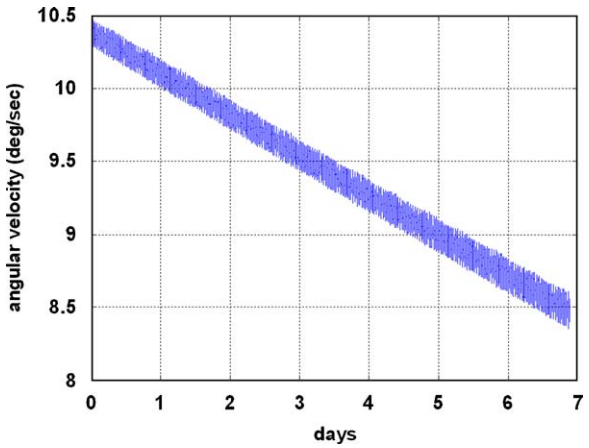

Fig. 16. Angular velocity damping after launch (two hysteresis rods per axis.

opposed to the material saturation magnetic flux of 1 T. The rod hysteresis loop and the material major hysteresis loops are shown in Fig. 14.

The rod performance in terms of the apparent permeability and demagnetization factor, can be evaluated comparing the material saturation flux intensity B_s and the measured rod saturation flux intensity B_s':

$$B_s = \mu_0\mu_r H_s, \quad B_s' = \mu_0\mu_r' H_s = \mu_0\frac{\mu_r}{1 + N\mu_r}H_s \tag{13}$$

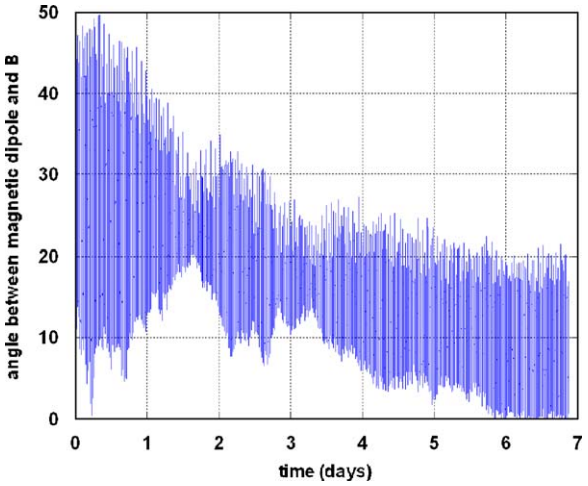

Fig. 17. Oscillation amplitude (two hysteresis rods per axis).

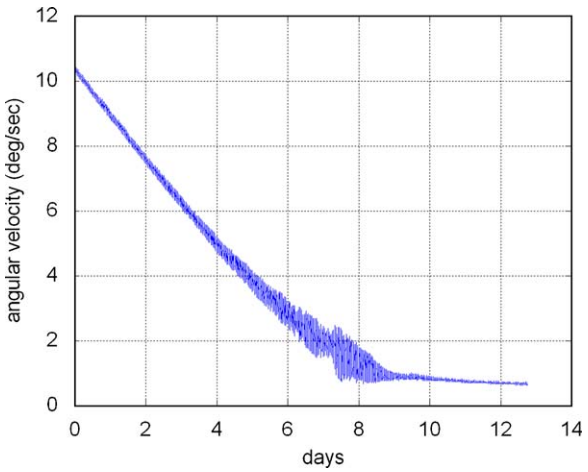

Fig. 18. Angular velocity damping after launch (eight rods per axis).

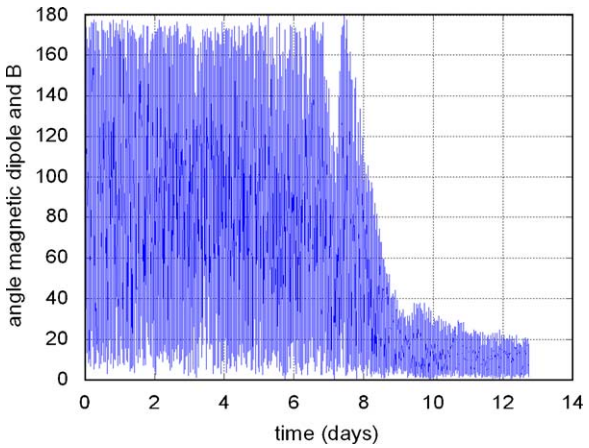

Fig. 19. Angle between the on-board magnetic dipole axis and Earth's magnetic field vector (eight rods per axis).

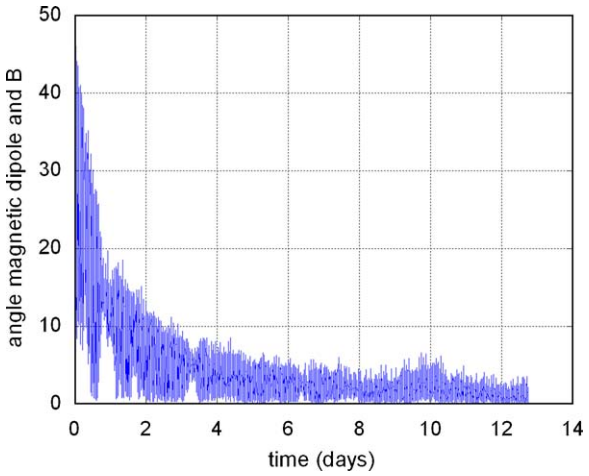

Fig. 20. Oscillation amplitude (eight rods per axis).

From these one gets

$$\mu_r' = \frac{B_s'}{B_s}\mu_r, \quad N = \frac{1}{\mu_r}\left(\frac{B_s}{B_s'} - 1\right) \tag{14}$$

The true permeability μ_r in (14) is the value at saturation, which can be obtained by the material manufacturer. The magnetic field strength at saturation is 100A/m. From the graph in Fig. 15 (see Ref. [18]), we find that $\mu_r = 10\,000$. Substituting in (14) the values of $B_s = 1\,\mathrm{T}$ and $B\prime_s = 0.025\,\mathrm{T}$, we get

$$\mu_r' = 250, \quad N = 3.9 \times 10^{-3} \tag{15}$$

The apparent permeability is lower than the predicted value of 300 (graphs in Fig. 4). This can be due to imperfections in the technological process of manufacturing and heat treatment. We can say that the bar is about 17% less efficient than expected from the theoretical sizing. This value is however completely acceptable for UNISAT-4, since it can be compensated by the inclusion of more bars in the system.

5. Numerical simulation

The attitude stabilization system performance has been assessed by numerical simulation of the attitude dynamics.

The rod mathematical model used for the simulation is the one described in Ref. [16], with the rod magnetic parameters evaluated experimentally from Fig. 13.

The results obtained with two hysteresis rods per axis and eight hysteresis rods per axis are compared.

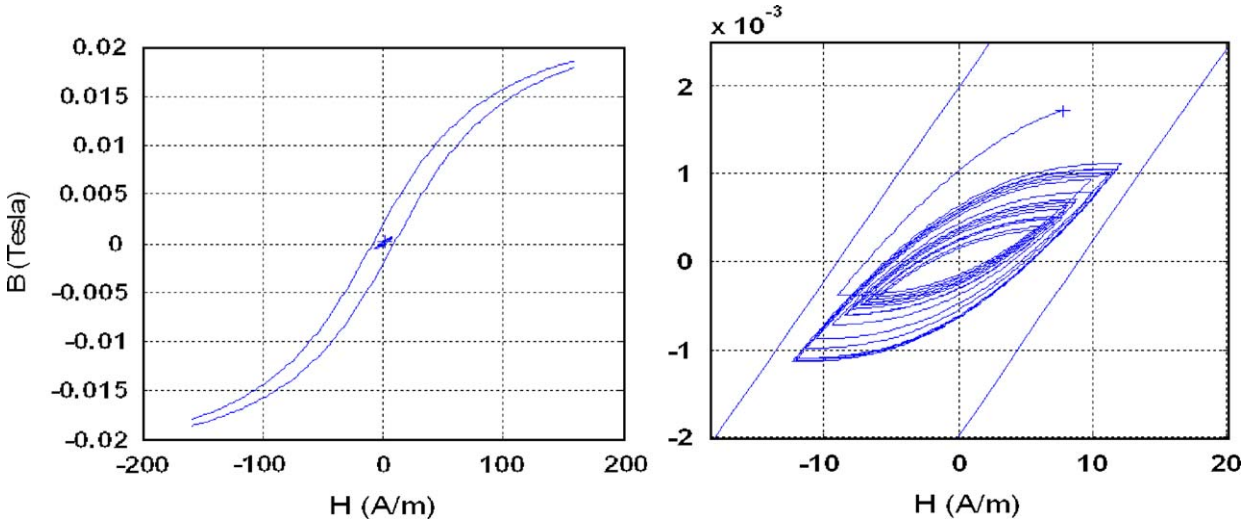

Fig. 21. Hysteresis rod loops during the satellite motion.

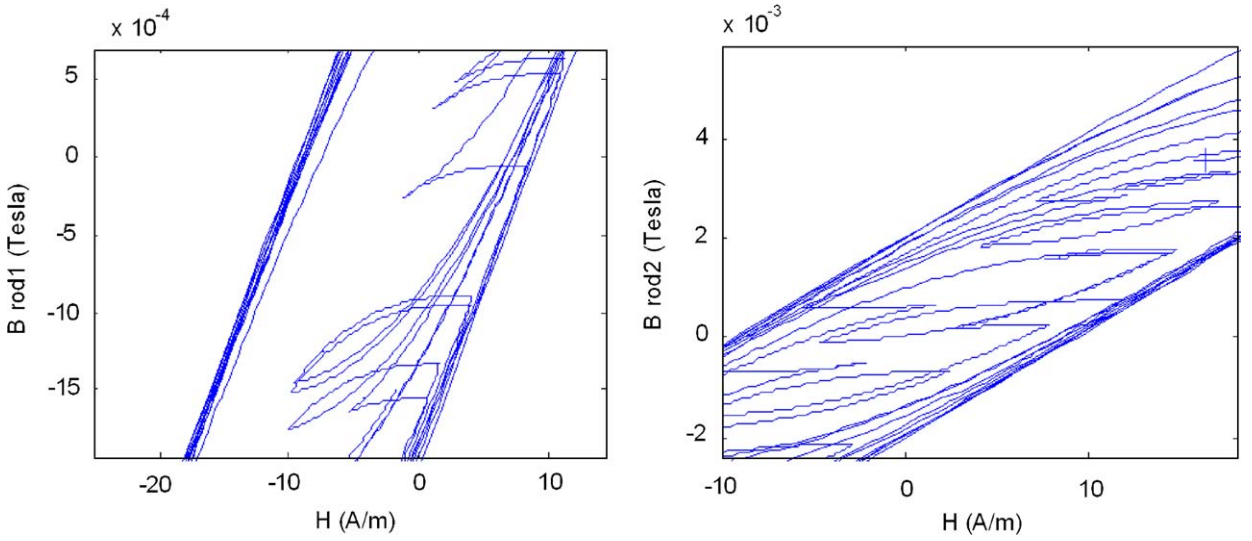

Fig. 22. "Partial loops" during the satellite motion.

At separation from the launcher the satellite angular velocity is in the order of 10°/s. The hysteresis rods dissipate the satellite kinetic energy, as shown in Fig. 16, slowing down the motion at a rate of about 0.3°/s/day. Then the satellite takes about 33 days to dissipate the initial kinetic energy at separation from the launcher and pass from the regime of rotations to the regime of oscillation around the Earth's magnetic field direction. In Fig. 17 it is shown how the satellite oscillation amplitude is damped out by the magnetic hysteresis rods. The oscillation amplitude decay rate is in the order of 5°/day. Assuming a worst case, initial amplitude of 180°, the satellite reaches steady state oscillation in about one month. Therefore, a total of about 2 months are necessary for spacecraft stabilization. The residual oscillation amplitude is about 20°.

The time necessary to stabilize the satellite can be reduced increasing the number of hysteresis rods.

The results obtained using eight hysteresis rods per axis are shown in Figs. 18–20. The angular velocity decay rate is about 1.25°/s/day, which is about four times more than the previous simulation, in accordance with the increased hysteresis rod total volume. In Fig. 19 we see that the transition from the regime of rotations to the regime of oscillation takes place after 8 days. In Fig. 20 we see that the oscillation amplitude reaches a stationary value of about 5° in approximately 6 days. Therefore, the time necessary for satellite stabilization with eight rods is 14 days.

Fig. 21 shows the hysteresis rod loops during the satellite motion, included in the major hysteresis cycle, indicating that the rod operates far from saturation.

Due to attitude motion, not always hysteresis loops are complete and centered in the *B–H* plane origin. An example of such "partial loops" is shown in Fig. 22.

6. Conclusions

The UNISAT-4 microsatellite passive magnetic attitude stabilization system design and test has been described and the permanent magnet and hysteresis rods sizing and manufacturing discussed. A procedure to determine the hysteresis rod parameters has been set up. The measurement results show that theoretical predictions of the hysteresis rod performance might be optimistic, since they do not take into account technological manufacturing process inaccuracies and other imperfections. It is shown that a system of eight bars per axis stabilizes the satellite in about 14 days from launch.

Acknowledgments

The Authors wish to acknowledge the support received by Prof. Filippo Graziani, Dean of the Scuola di Ingegneria Aerospaziale and all the professors and students directly or indirectly involved in the UNISAT program.

Appendix A. Expressions of hysteresis rods demagnetization factor

Following are the expressions of the demagnetization factors found in Refs [12–14].

In Ref. [12] the expression for a square cross-section bar is given:

$$\pi N = \left(m - \frac{1}{m}\right)\ln\left(\frac{\sqrt{m^2+2}+1}{\sqrt{m^2+2}-1}\right) + \frac{2}{m}\ln(\sqrt{2}+1) + m\ln\left(\frac{\sqrt{m^2+2}-1}{\sqrt{m^2+2}+1}\right) + 2\arctan\left(\frac{1}{m\sqrt{m^2+2}}\right) + \frac{2(1-m^2)}{3m}\sqrt{m^2+2} + \frac{2(1-m^3)}{3m} - \frac{2^{3/2}}{3m} + \frac{2}{3}\sqrt{m^2+1}\left(2m - \frac{1}{m}\right)$$

In Ref. [13], we find the following simplified expression of N for rectangular rods:

$$N = \frac{1}{1+2m}$$

In Ref. [14], we find the following simplified expression of N for prolate ellipsoids ($\chi = \infty$):

$$N = \frac{1}{m^2}\ln(2m-1)$$

and for long cylinders:

$$N = \frac{1}{m^2}\ln\left(2m - \frac{3}{2}\right)$$

References

[1] F. Graziani, F. Santoni, The UNISAT program for space education, Keynote invited paper, in: The 23rd International Symposium on Space Technology and Science, Matsue, Japan, 26 May–2 June, 2002.
[2] F. Santoni, F. Graziani, Space education using university microsatellites, in: The 53rd International Astronautical Congress, Paper IAC-02-P.P.03, Houston, TX, USA, 10–19 October 2002.
[3] F. Graziani, M. Ferrante, G.B. Palmerini, F. Santoni, P. Tortora, UNISAT program, a university tool for space education, in: The 51st International Astronautical Congress, Paper IAF-00-P.2.07, Rio de Janeiro, Brasil, 2–6 October 2000.
[4] F. Graziani, F. Santoni, F. Piergentili, F. Bulgarelli, M. Sgubini, S. Bernardini, Manufacturing and launching student-made microsatellites: "hands-on" education at the University of Roma, in: The 55th International Astronautical Congress, Paper IAC-04-P.5.A.02, Vancouver, Canada, October 2004.
[5] F. Santoni, F. Piergentili, F. Bulgarelli, F. Graziani, The Unisat Program: Lessons Learned and Achieved Results, in: The 57th International Astronautical Congress, Paper IAC-06-E1.1.10, Valencia, Spain, October 2006.
[6] F. Piergentili, F. Graziani, UNISAT A low cost, autonomous deorbiting system for microsatellites: SIRDARIA, in: The 57th International Astronautical Congress, Paper IAC-06-B6.4.07, Valencia, Spain, October 2006.
[7] M.L. Battagliere, F. Piergentili, G. Vannaroni, F. Graziani, Triple probe system for in situ ionospheric plasma monitoring,

in: XVIII Congresso Nazionale A.I.D.A.A., Volterra, Italy, 19–22 September 2005.

[8] M. Ovchinnikov, V. Pen'kov, O. Norberg, S. Barabash, Attitude control system for the first Swedish nanosatellite "MUNIN", Acta Astronautica 46 (2000).

[9] B.V. Rauschenbakn, M. Ovchinnikov, S. McKenna-Lawlor, Essential spaceflight dynamics and magnetospherics, The Space Technology Library, vol. 15, Kluwer Academic Publishers, Dordrecht, 2002.

[10] F. Santoni, F. Piergentili, UNISAT-3 attitude determination using solar panel and magnetometer data, Paper IAC-05-C1.2.06, in: The 56th International Astronautical Congress, Fukuoka, Japan, 17–21 October 2005.

[11] R.M. Bozorth, Ferromagnetism, Van Nostrand, Reinhold, New York, 1951.

[12] A. Aharoni, Demagnetizing factors for rectangular ferromagnetic prisms, Journal of Applied Physics 83 (6) (1998) 3432–3434.

[13] M. Sato, Y. Ishii, Simple and approximate expressions of demagnetizing factors of uniformly magnetized rectangular rod and cylinder, Journal of Applied Physics 66 (2) (1989) 983–985.

[14] C.X. Chen, Demagnetizing factors of long cylinders with infinite susceptibility, Journal of Applied Physics 89 (6) (2001) 3413–3415.

[15] R.E. Fishell, Magnetic damping of the angular motion of Earth satellites, ARS Journal (1961) 1210–1217.

[16] R.R. Kumar, D.D. Mazanek, M.L. Heck, Simulation and shuttle hitchhiker validation of passive satellite aerostabilization, Journal of Spacecraft and Rockets 32 (5) (1995).

[17] J. Buck, Automatic Hysteresisgraph Speeds Accurate Analysis of Soft Magnetic Materials, Presented at PCIM, Walker Scientific Inc. ⟨http://www.walkerscinetific.com/buck.pdf⟩.

[18] Vacuumschmelze GMBH & Co. KG, Soft Magnetic and Semi-finished Products, Edition 2002.